

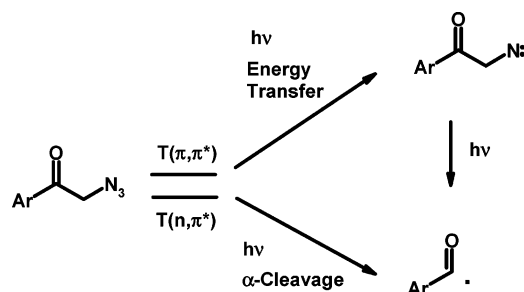
Competition between α -Cleavage and Energy Transfer in α -Azidoacetophenones

Sivaramakrishnan Muthukrishnan,[†] Sarah M. Mandel,[†] John C. Hackett,[‡]
Pradeep N. D. Singh,[†] Christopher M. Hadad,[‡] Jeanette A. Krause,[†] and
Anna D. Gudmundsdóttir^{*,†}

Department of Chemistry, University of Cincinnati, Cincinnati, Ohio 45221-0172 and Department of
Chemistry, The Ohio State University, Columbus, Ohio 43210-1173

Anna.Gudmundsdottir@uc.edu

Received October 17, 2006



Molecular modeling demonstrates that the first excited state of the triplet ketone (T_{1K}) in azide **1b** has a (π, π^*) configuration with an energy that is 66 kcal/mol above its ground state and its second excited state (T_{2K}) is 10 kcal/mol higher in energy and has a (n, π^*) configuration. In comparison, T_{1K} and T_{2K} of azide **1a** are almost degenerate at 74 and 77 kcal/mol above the ground state with a (n, π^*) and (π, π^*) configuration, respectively. Laser flash photolysis (308 nm) of azide **1b** in methanol yields a transient absorption ($\lambda_{\max} = 450$ nm) due to formation of T_{1K} , which decays with a rate of 2.1×10^5 s⁻¹ to form triplet alkylnitrene **2b** ($\lambda_{\max} = 320$ nm). The lifetime of nitrene **2b** was measured to be 16 ms. In contrast, laser flash photolysis (308 nm) of azide **1a** produced transient absorption spectra due to formation of nitrene **2a** ($\lambda_{\max} = 320$ nm) and benzoyl radical **3a** ($\lambda_{\max} = 370$ nm). The decay of **3a** is 2×10^5 s⁻¹ in methanol, whereas nitrene **2a** decays with a rate of ~ 91 s⁻¹. Thus, T_{1K} (π, π^*) in azide **1b** leads to energy transfer to form nitrene **2b**; however, α -cleavage is not observed since the energy of T_{2K} (n, π^*) is 10 kcal/mol higher in energy than T_{1K} , and therefore, T_{2K} is not populated. In azide **1a** both α -cleavage and energy transfer are observed from T_{1K} (n, π^*) and T_{2K} (π, π^*), respectively, since these triplet states are almost degenerate. Photolysis of azide **1a** yields mainly product **4**, which must arise from recombination of benzoyl radicals **3a** with nitrenes **2a**. However, products studies for azide **1b** also yield **4b** as the major product, even though laser flash photolysis of azide **1b** does not indicate formation of benzoyl radical **3b**. Thus, we hypothesize that benzoyl radicals **3** can also be formed from nitrenes **2**. More specifically, nitrene **2** does undergo α -photocleavage to form benzoyl radicals and iminyl radicals. The secondary photolysis of nitrenes **2** is further supported with molecular modeling and product studies.

I. Introduction

The high-spin properties of triplet nitrenes provide a potential application as organic magnets, and such desires have regenerated interest in these intermediates.¹ However, triplet alkylnitrenes have only been studied sporadically, presumably because

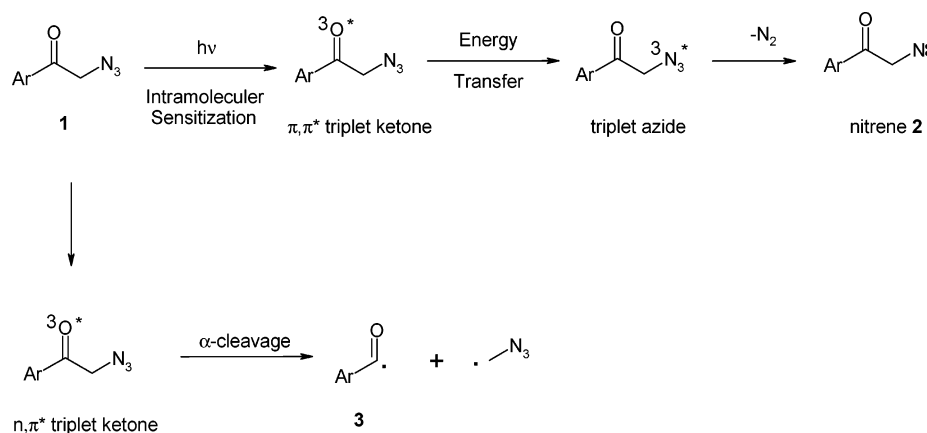
direct irradiation or thermal activation of alkyl azides does not lead to formation of triplet alkylnitrene intermediates at ambient temperature.^{2,3} Rather, triplet sensitization must be used to form triplet alkylnitrenes from alkyl azides.^{4,5} Recently, we demon-

[†] University of Cincinnati.

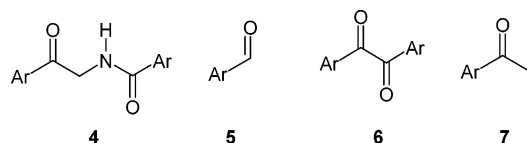
[‡] The Ohio State University.

(1) (a) *Magnetic Properties of Organic Materials*; Lahti, P. M., Ed.; Marcel Dekker, Inc.: New York, 1999. (b) Tomioka, H. Triplet Carbenes. In *Reactive Intermediate Chemistry*; Moss, R. A., Platz, M. S., Jones, M., Jr., Eds.; John Wiley & Sons, Inc.: Hoboken, NJ, 2004; pp 501–592.

SCHEME 1



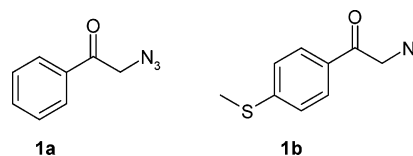
SCHEME 2



strated that photolysis of azides **1** (Scheme 1) yields triplet alkylnitrene intermediates **2** via intramolecular triplet sensitization from the ketone chromophore to the azido moiety.^{4a} By photolyzing azides **1** with light above 300 nm, only the aryl ketone chromophore absorbs the light and forms the first excited singlet state of the ketone, which undergoes efficient intersystem crossing to the triplet ketone.⁶ Energy transfer from the triplet ketone to the azido moiety results in formation of triplet nitrene intermediates.

In competition with energy transfer, azide **1** can undergo α -cleavage to form benzoyl radical **3** and the azidomethyl ($\text{N}_3\text{-CH}_2\cdot$) radical. The energy transfer in the α -azidoacetophenones must come from the (π, π^*) state of the triplet ketone since the α -cleavage occurs from the (n, π^*) state.⁷ Product studies have shown that irradiating azide **1** yields mainly **4** and a small amount of benzaldehyde (**5**), benzyl (**6**), and acetophenone (**7**) derivatives. Presumably, triplet alkylnitrene **2** reacts with benzoyl radicals **3** and the resulting radical abstracts a hydrogen atom from the solvent to form **4** (Scheme 2). However, photolysis of α -azido-(*p*-cyano)-acetophenone, which has the

SCHEME 3



first excited state of the triplet ketone (T_{1K}) with a (π, π^*) configuration, gives the same photoproducts as α -azidoacetophenone, which has T_{1K} with the (n, π^*) configuration.

Hence, we set out to study how the energies of the two (n, π^*) and (π, π^*) configurations, T_{1K} and T_{2K} , in α -azidoacetophenone derivatives affect the corresponding product formation, and this will be investigated by comparing the photochemistry of azides **1a** and **1b** (Scheme 3). On the basis of the similarity of azides **1** with the analogous valerophenone derivatives, we expect azide **1a** to have almost degenerate T_{1K} and T_{2K} whereas T_{1K} (π, π^*) in azide **1b** is expected to be almost 10 kcal/mol lower in energy than T_{2K} (n, π^*).⁸

In this article, we describe how experimental laser flash photolysis and product studies along with molecular modeling reveal that azide **1a** undergoes both α -cleavage and energy transfer to form benzoyl radical **3a** and triplet alkylnitrene **2a**, whereas azide **1b** selectively forms triplet alkylnitrene **2b**. However, triplet alkylnitrenes **2** are photoreactive themselves and undergo α -cleavage to form benzoyl and iminyl radicals.

II. Results

A. Phosphorescence Spectra. We measured the phosphorescence of **7b** and azide **1b** at 77 K in ethanol glasses (Figure 1) under identical experimental conditions (0.6 mmol, $\lambda_{\text{ex}} = 353$ nm). We did not observe any phosphorescence for azide **1a**, presumably since the triplet ketone is efficiently quenched by intramolecular energy transfer to the azido moiety.^{4a} Ketone **7b** and azide **1b** show structureless phosphorescence which is typical⁹ for triplet ketones with a (π, π^*) configuration. Since **7b** and **1b** have similar UV absorption spectra (Supporting Information) and their phosphorescence spectra were recorded under the same conditions, we compared their yield of emission

(2) Platz, M. S. Nitrenes. In *Reactive Intermediate Chemistry*; Moss, R. A., Platz, M. S., Jones, M., Jr., Eds.; John Wiley & Sons, Inc.: Hoboken, NJ, 2004; pp 375–461.

(3) (a) Barash, L.; Wasserman, E.; Yager, W. A. *J. Am. Chem. Soc.* **1967**, 89, 3931. (b) Radziszewski, J. G.; Downing, J. W.; Jawdosiuk, M.; Kovacic, P.; Michl, J. *J. Am. Chem. Soc.* **1985**, 107, 594. (c) Carrick, P. G.; Brazier, C. R.; Bernath, P. F.; Engelking, P. C. *J. Am. Chem. Soc.* **1987**, 109, 5100. (g) Ferrante, R. F. *J. Chem. Phys.* **1987**, 86, 25. (e). Gritsan, N. P.; Likhovotvorik, I.; Zhu, Z.; Platz, M. S. *J. Phys. Chem. A* **2001**, 105, 3039.

(4) (a) Mandel, S. M.; Singh, P. N. D.; Robinson, R. M.; Zhu, Z.; Franz, R.; Ault, B. S.; Gudmundsdóttir, A. D. *J. Org. Chem.* **2003**, 68, 7951. (b) Mandel, S. M.; Krause Bauer, J. A.; Gudmundsdóttir, A. D. *Org. Lett.* **2001**, 3, 523.

(5) Klima, R. F.; Gudmundsdóttir, A. D. *J. Photochem. Photobiol., A* **2003**, 162, 239.

(6) McGarry, P. F.; Doubleday, C. E., Jr.; Wu, C.-H.; Staab, H. A.; Turro, N. J. *J. Photochem. Photobiol., A* **1994**, 77, 109.

(7) (a) Turro, J. *Modern Molecular Photochemistry*; University Science Books: Sausalito, CA, 1991; Chapter 7. (b) Garcia-Garibay, M. A.; Campos, L. M. Photochemical decarbonylation of ketones: recent advances and reactions in crystalline solids. In *CRC Handbook of Organic Photochemistry and Photobiology*, 2nd ed.; Horspool, W., Lenci, F., Eds.; CRC Press: Boca Raton, FL, 2004; Chapter 48.

(8) Wagner, P. J.; Kemppainen, A. E.; Schott, H. N. *J. Am. Chem. Soc.* **1973**, 95, 5604.

(9) (a) Turro, J. *Modern Molecular Photochemistry*; University Science Books: Sausalito, CA, 1991; Chapter 5. (b) Becker, R. *Theory and Interpretation of Fluorescence and Phosphorescence*; Wiley: New York; 1969.

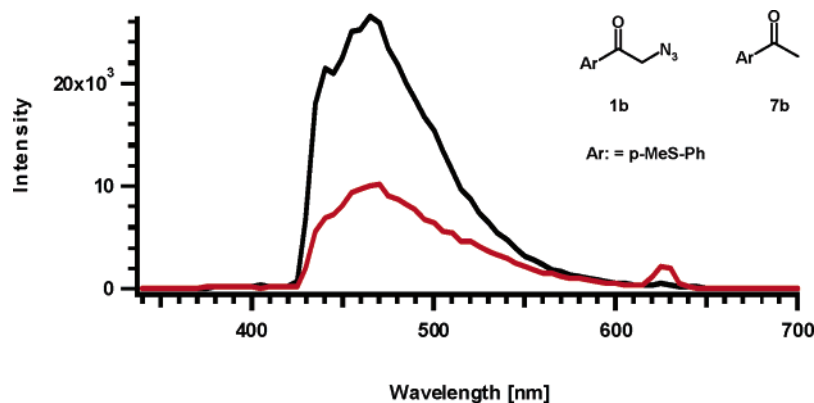
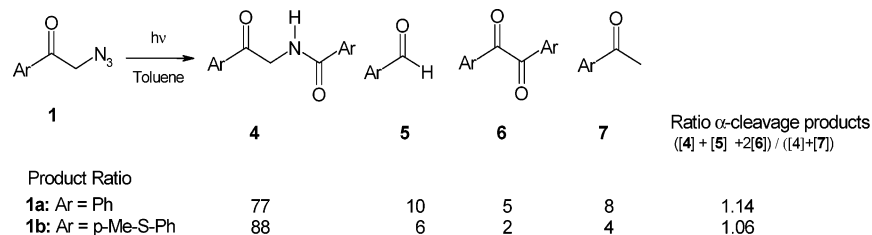
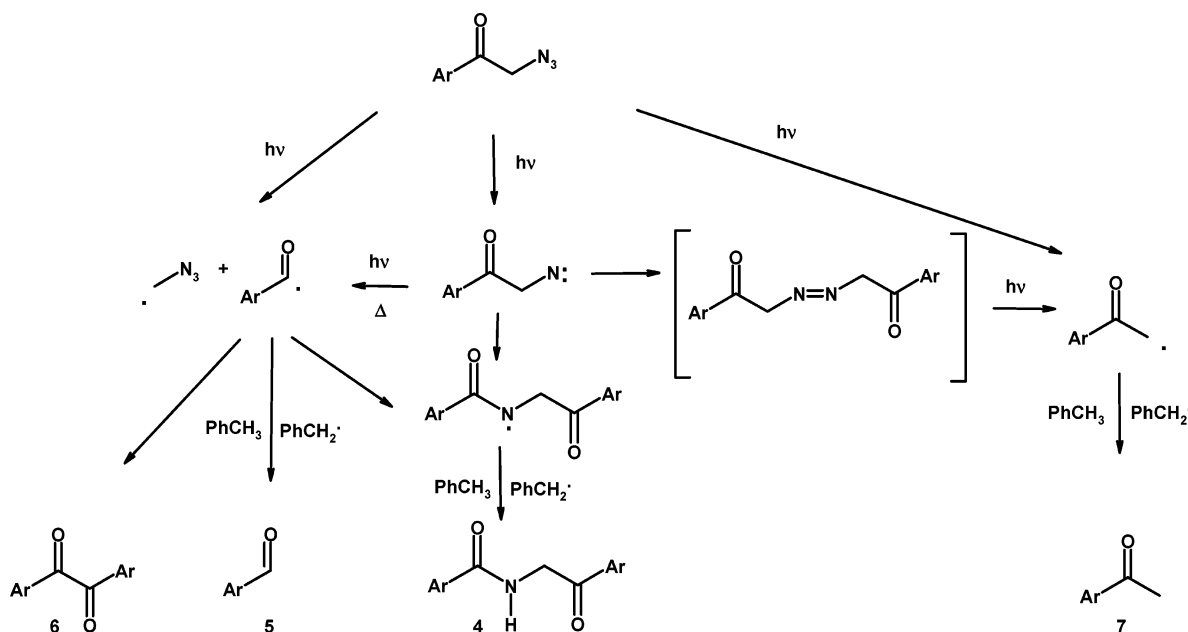


FIGURE 1. Phosphorescence spectra of azides **1b** (red) and **7b** (black).

SCHEME 4



SCHEME 5



and found that the yield for azide **1b** is less than for **7b**, indicating that some of the phosphorescence is quenched by energy transfer to the azido group. From the phosphorescence spectra we can estimate that the energy of the triplet ketone in **7b** and azide **1b** are similar or ~ 64 kcal/mol.¹⁰

B. Product Studies. Product studies from the photolysis of **1a** have been described previously but are included here for comparison.⁴ Photolysis of azides **1a** and **1b** in toluene, under the same experimental conditions, yields one major product **4**.

In addition, smaller amounts of benzaldehyde **5**, benzil **6**, and acetophenone **7** are formed as well (Scheme 4). Similar photoproduct ratios are observed for azides **1a** and **1b**. As mentioned before, product **4** must come from the initially generated nitrene **2** being able to trap benzoyl radical **3** and the resulting radical subsequently abstracting an H atom from the solvent (Scheme 5). Similarly, **5** and **6** presumably come from the benzoyl radical reacting with toluene or undergoing dimerization. It is possible that nitrene **2** dimerizes to form the azodimer that subsequently absorbs another photon to form acetophenone radicals, which abstract a hydrogen atom from the solvent to form **7**. It is, however, possible that azide **1** undergoes β -cleavage to form azido and acetophenonyl radicals.

(10) Murow, S. L. Carmichael, I.; Hug, G. L. *Handbook of Photochemistry*, Marcel Dekker: New York, 1993.

(11) Wilson, R. M.; Patterson, W. S.; Austen, S. C.; Ho, D. M.; Krause-Bauer, J. A. *J. Am. Chem. Soc.* **1995**, *117*, 7820.

Interestingly, azide **1b** yields similar quantity of products **4**, **5**, and **6** as azide **1a**, even though they can be attributed to benzoyl radical formation. Thus, we theorized whether nitrenes **2** can fall apart to yield benzoyl radical **3** either thermally or photochemically.

C. Molecular Modeling. All structures were optimized using Gaussian03¹² at the B3LYP level of theory and with the 6-31+G(d) basis set,¹³ unless otherwise noted. We optimized the ground-state (S_0) configuration of azides **1**, triplet nitrenes **2**, benzoyl radicals **3**, azidomethyl radical, and methylene iminyl radical. We calculated the IR spectra of these optimized structures from vibrational frequency analyses at the same level of theory. The optimized geometries of azides **1a** and **1b** are very similar; both molecules are relatively flat with the exception of the azido moiety being twisted out of the plane of the phenyl ring, as revealed by the torsion angle between C7–C8–N1–N2 being 62° for both **1a** and **1b** (Figure 2 and 3). Furthermore, the X-ray structure of azide **1b** is similar to its optimized structure (see Supporting Information and Figure 4). In the X-ray structure, both the carbonyl group and Me–S substituents are rotated slightly out of the plane of the phenyl ring, presumably to accommodate for the crystal packing arrangement of the molecule. The twisting of **1b** in the crystal lattice can be seen by the torsion angle between C6–C1–C7–O1 and C9–S1–C4–C5, which are 11.8° and –16.3°, respectively.

We used time-dependent density functional theory (TD-DFT)¹⁴ to estimate the vertical excitation energies of T_{1K} and T_{2K} for azides **1a** and **1b** (Table 1) using the geometry for the S_0 state. In azide **1a**, T_{1K} is located 75 kcal/mol above the ground state. Visualization of the molecular orbitals for the major components of the electronic excitation revealed that this T_{1K} state is dominated by a (n,π^*) configuration as expected, and it is about 1 kcal/mol more stable than T_{2K} , which has a (π,π^*) configuration. Solvation¹⁵ does not significantly change the relative energies of T_{1K} and T_{2K} in azide **1a** (Table 1). The calculated energy difference between T_{1K} and T_{2K} in azide **1a** fits well with what has been estimated for valerophenone and

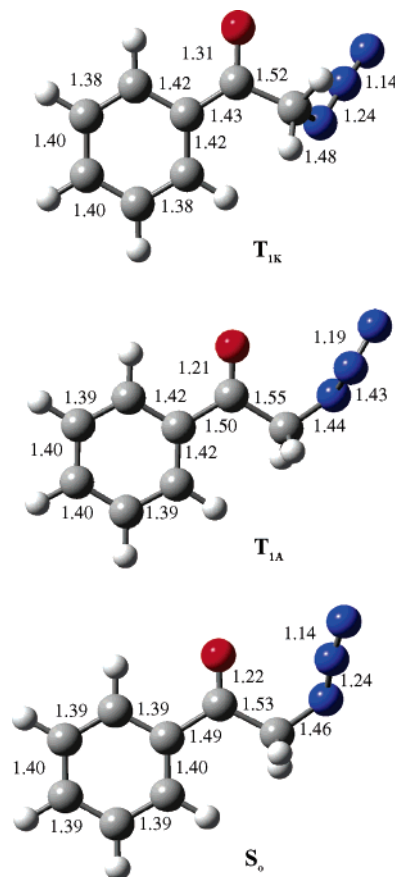


FIGURE 2. Optimized S_0 , T_{1A} , and T_{1K} geometries of azide **1a** at the RB3LYP (S_0) and UB3LYP (T_{1A} and T_{1K}) levels of theory. Bond lengths are in Ångstroms.

butyrophenone derivatives.^{16,17} TD-DFT calculations estimated the vertical excitation energy of T_{1K} of azide **1b** to be 66 kcal/mol above the ground state and have a (π,π^*) configuration; furthermore, T_{2K} is 10 kcal/mol higher in energy than T_{1K} . This is similar to the estimated energy difference between T_{1K} (π,π^*) and T_{2K} (n,π^*) in the analogous thiomethyl valerophenone.⁸

We optimized the triplet excited states of the azide moiety, T_{1A} , in azides **1** at the unrestricted B3LYP/6-31+G(d) level and found that T_{1A} was located 45 kcal/mol above the ground state. The N1–N2–N3 bond in T_{1A} has a bond angle of ~120.7°, and the N1–N2 bond length is 1.43 Å (Figure 2 and 3), whereas in the ground state of azides **1a,b**, the N1–N2 bond length is 1.23 Å. As a reflection of the increased length of the N1–N2 bond, the calculated IR spectrum of T_{1A} does not have an azide stretching vibration at ~2100 cm^{-1} , as seen for azides **1a,b**, but rather the N–N stretch is calculated to be ~1720 cm^{-1} . T_{1A} can be assigned to the (n,π^*) configuration of the triplet azides based on visualization of the molecular orbitals (see Supporting Information).

(12) Frisch, M. J.; Trucks, G. W.; Schlegel, H. B.; Scuseria, G. E.; Robb, M. A.; Cheeseman, J. R.; Montgomery, J. A., Jr.; Vreven, T.; Kudin, K. N.; Burant, J. C.; Millam, J. M.; Iyengar, S. S.; Tomasi, J.; Barone, V.; Mennucci, B.; Cossi, M.; Scalmani, G.; Rega, N.; Petersson, G. A.; Nakatsuji, H.; Hada, M.; Ehara, M.; Toyota, K.; Fukuda, R.; Hasegawa, J.; Ishida, M.; Nakajima, T.; Honda, Y.; Kitao, O.; Nakai, H.; Klene, M.; Li, X.; Knox, J. E.; Hratchian, H. P.; Cross, J. B.; Adamo, C.; Jaramillo, J.; Gomperts, R.; Stratmann, R. E.; Yazyev, O.; Austin, A. J.; Cammi, R.; Pomelli, C.; Ochterski, J. W.; Ayala, P. Y.; Morokuma, K.; Voth, G. A.; Salvador, P.; Dannenberg, J. J.; Zakrzewski, V. G.; Dapprich, S.; Daniels, A. D.; Strain, M. C.; Farkas, O.; Malick, D. K.; Rabuck, A. D.; Raghavachari, K.; Foresman, J. B.; Ortiz, J. V.; Cui, Q.; Baboul, A. G.; Clifford, S.; Cioslowski, J.; Stefanov, B. B.; Liu, G.; Liashenko, A.; Piskorz, P.; Komaromi, I.; Martin, R. L.; Fox, D. J.; Keith, T.; Al-Laham, M. A.; Peng, C. Y.; Nanayakkara, A.; Challacombe, M.; Gill, P. M. W.; Johnson, B.; Chen, W.; Wong, M. W.; Gonzalez, C.; Pople, J. A. *Gaussian 03*, Revision A.1; Gaussian, Inc.: Pittsburgh, PA, 2003.

(13) (a) Becke, A. D. *J. Chem. Phys.* **1993**, *98*, 5648. (b) Lee, C.; Yang, W.; Parr, R. G. *Phys. Rev. B* **1988**, *37*, 785.

(14) (a) *Density Functional Methods in Chemistry*; Labanowski, J., Ed.; Springer-Verlag: Heidelberg, 1991. (b) Parr, R. G.; Weitao, Y. *Density-Functional Theory in Atoms and Molecules*; Oxford University Press: New York, 1989. (c) Bauernschmitt, R. *Chem. Phys. Lett.* **1996**, *256*, 454. (d) Stratmann, R. *J. Chem. Phys.* **1998**, *109*, 8218. (e) Foresman, J. *J. Phys. Chem.* **1992**, *96*, 135.

(15) (a) Tomasi, J.; Mennucci, B.; Cammi, R. *Chem. Rev.* **2005**, *105*, 2999. (b) Mennucci, B.; Cancès, E.; Tomasi, J. *J. Phys. Chem. B* **1997**, *101*, 10506. (c) Cancès, E.; Mennucci, B. *J. Chem. Phys.* **2001**, *114*, 4744. (d) Tomasi, J.; Persico, M. *Chem. Rev.* **1994**, *94*, 2027. (e) Cramer, C. J.; Truhlar, D. J. *Chem. Rev.* **1999**, *99*, 2161.

(16) (a) He, H.-Y.; Fang, W.-H.; Phillips, D. L. *J. Phys. Chem. A* **2004**, *108*, 5386. (b) Fang, W.-H.; Phillips, D. L. *Chem. Phys. Chem.* **2002**, *3*, 889. (c) Fang, W.-H.; Phillips, D. L. *J. Theor. Comput. Chem.* **2003**, *2*, 23.

(17) (a) Wagner, P. J. Abstraction of γ -hydrogens by excited carbonyls. In *Molecular and Supramolecular Photochemistry*; Griesbeck, A. G., Mattay, J., Eds.; Marcel Dekker: New York, 2005; Chapter 2. (b) Wagner, P. J. In *CRC Handbook of Organic Photochemistry and Photobiology*; Horspool, W. M., Song, P.-S., Eds.; CRC Press: Boca Raton, FL, 1995; Chapter 52. (c) Wagner, P. J. Photoinduced Hydrogen Atom Abstraction by Carbonyl Compounds. In *Organic Photochemistry*; Padwa, A., Ed.; Marcel Dekker: New York, 1991; Vol. 11, Chapter 4, p 227.

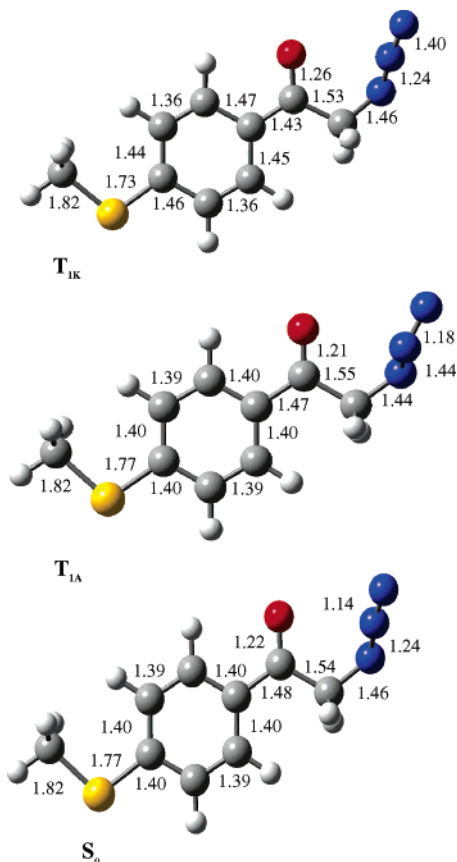


FIGURE 3. Optimized S_0 , T_{1A} , and T_{1K} geometries of azide **1b** at the RB3LYP (S_0) and UB3LYP (T_{1A} and T_{1K}) levels of theory. Bond lengths are in Ångstroms.

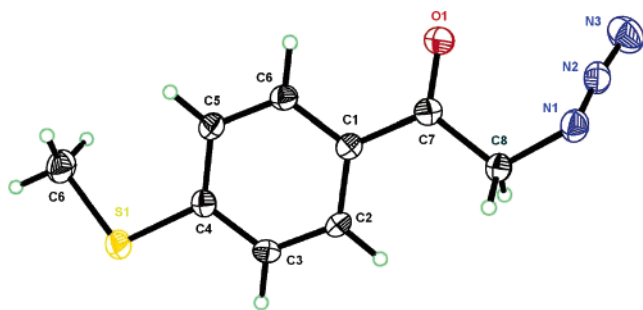


FIGURE 4. Crystal structure of azide **1b**.

We also optimized T_{1K} for azide **1a** and found that it is located 66 kcal/mol above the S_0 ground state of azide **1a**. In T_{1K} , the $N_1-N_2-N_3$ bond is almost linear (173°) and the calculated vibrational stretching frequency for the azide group is 2218 cm^{-1} , which is similar to what was calculated for the ground state of azide **1a** (Figure 2). The C–O bond has lengthened from 1.22 \AA in the ground state to 1.31 \AA , and it has a stretching vibration at 1380 cm^{-1} . The progression of the C–O bond and its IR vibration fits well with what has been observed for triplet aryl ketones with a (n,π^*) configuration.^{16,19} The energy of T_{1K} obtained from the (vertical) TD-DFT calculation and the optimized structure at the UB3LYP level differ by almost 9

(18) Ahlrichs, R.; Bär, M.; Häser, M.; Horn, H.; Kölmel, C. *Chem. Phys. Lett.* **1989**, 162, 165.

(19) Srivastava, S.; Yourd, E.; Toscano, J. P. *J. Am. Chem. Soc.* **1998**, *120*, 6173.

TABLE 1. Comparison of the Calculated Energies for the Triplet Excited States of Azides 1a,b

		azide 1a		azide 1b	
state	method	configuration	energy (kcal/mol) ^a	configuration	energy (kcal/mol)
T _{1K}	TD-B3LYP	(n,π*)	75.0 (76.1)	(π,π*)	65.6 (65.1)
	optimized ^b		66.0 (67.2)		64.0 (63.0)
	TURBOMOLE ^c		65.8		
T _{2K}	TD-B3LYP	(π,π*)	76.3 (77.4)	(n,π*)	76.0 (78.2)
T _{1A}	optimized ^b	(n,π*)	45.0	(n,π*)	45.1

^a Numbers in parentheses are calculated energies at the PCM level with toluene as a solvent. ^b Optimized using Gaussian03 at the UB3LYP level of theory. ^c Optimized using TURBOMOLE with analytical derivatives at the TD-B3LYP level of theory.

^a Numbers in parentheses are calculated energies at the PCM level with toluene as a solvent. ^b Optimized using Gaussian03 at the UB3LYP level of theory. ^c Optimized using TURBOMOLE with analytical derivatives at the TD-B3LYP level of theory.

kcal/mol. In order to clarify this difference, we also optimized T_{1K} for azides **1a** using TURBOMOLE and utilized the analytical first derivative of TD-DFT with the B3LYP functional as implemented in this program.¹⁸ For these calculations, the 6-31+G(d) basis set was used with the B3LYP DFT method. However, the geometry and energy of T_{1K} of azides **1a** were almost identical using the optimized TD-B3LYP and UB3LYP methods. We compared the optimization of T_{1K} in azide **1a** with the calculated energy of T_{1K} in acetophenone. TD-B3LYP estimates the energy of T_{1K} to be 74 kcal/mol, which is in excellent agreement with the measured energy of 74 kcal/mol for the triplet ketone in acetophenone.¹⁰ In comparison, optimization of T_{1K} in acetophenone using UB3LYP/6-31+G(d) gave the adiabatic energy of T_{1K} (n,π^*) as 69 kcal/mol, which is 5 kcal/mol lower than its measured energy.¹⁰ Thus, UB3LYP appears to underestimate the adiabatic energy of T_{1K} in acetophenone derivatives with the (n,π^*) configuration, whereas the TD-B3LYP calculations estimate these energies more accurately.

In order to evaluate whether solvation was the origin of the difference between the calculated and experimental energies, we did some other calculations in which a methanol molecule was explicitly hydrogen bonded to the carbonyl group of T_{1K} and S₀ of azide **1a**, so as to estimate how hydrogen bonding of the solvent might affect their energies. However, the energy difference (67 kcal/mol) between S₀ and T_{1K} in azide **1a** was very similar to that in the gas phase.

UB3LYP optimization of the triplet ketone, T_{1K} , in azide **1b** shows that the C=O bond in T_{1K} is 1.26 Å, and its stretching vibration occurs at 1478 cm^{-1} , indicating that the C–O bond has more double-bond character than for T_{1K} in azide **1a**. Furthermore, the aromatic carbon–carbon bonds in the phenyl ring are lengthened (Figure 3), as expected for triplet aryl ketones with a (π, π^*) configuration.^{16,19} The energy of the optimized triplet ketone is 63 kcal/mol above its ground state. Thus, the energies of the optimized structure T_{1K} and the TD-DFT calculation matched well with the energy of T_{1K} obtained from the phosphorescence spectrum of azide **1b**.

We optimized the geometry of nitrenes **2** and used TD-B3LYP to estimate the first and second excited triplet states of the ketone moiety in the molecule and found that the T_1 and T_2 of the nitrenes have energies and configurations like their corresponding azide precursors. We also used the TD-B3LYP level to estimate the absorption spectra of nitrenes **2a,b** (Table 2).

Similarly, we optimized the geometry of benzoyl radicals **3** and obtained their IR spectra. TD-DFT calculations were used to estimate the absorption spectra as shown in Table 2.

TABLE 2. Major Absorption Spectral Features (nm, Oscillator Strength) for **2** and **3**^a

		electronic transition above 300 nm				
2a	gas phase	386 (0.001)	344 (0.0096)	342 (0.0003)	317 (0.0015)	
	MeOH	378 (0.0001)	362 (0.0002)	355 (0.0142)	308 (0.0243)	306 (0.0113)
2b	gas phase	435 (0.0002)	356 (0.0321)	342 (0.0003)	318 (0.0013)	307 (0.1904)
	MeOH	450 (0.0038)	399 (0.0399)	358 (0.0350)	322 (0.2030)	320 (0.2411)
3a	gas phase	362 (0.0002)	335 (0.001)	313 (0.0001)		
	MeOH	364 (0.0004)	326 (0.0005)	300 (0.0002)		
3b	gas phase	419 (0.0009)	347 (0.0001)	332 (0.0001)	303 (0.0272)	300 (0.3225)
	MeOH	428 (0.0020)	364 (0.0001)	314 (0.3691)	312 (0.0952)	309 (0.0001)

^a Number in parentheses is the calculated oscillator strength (*f*) for the electronic transition in nanometers.

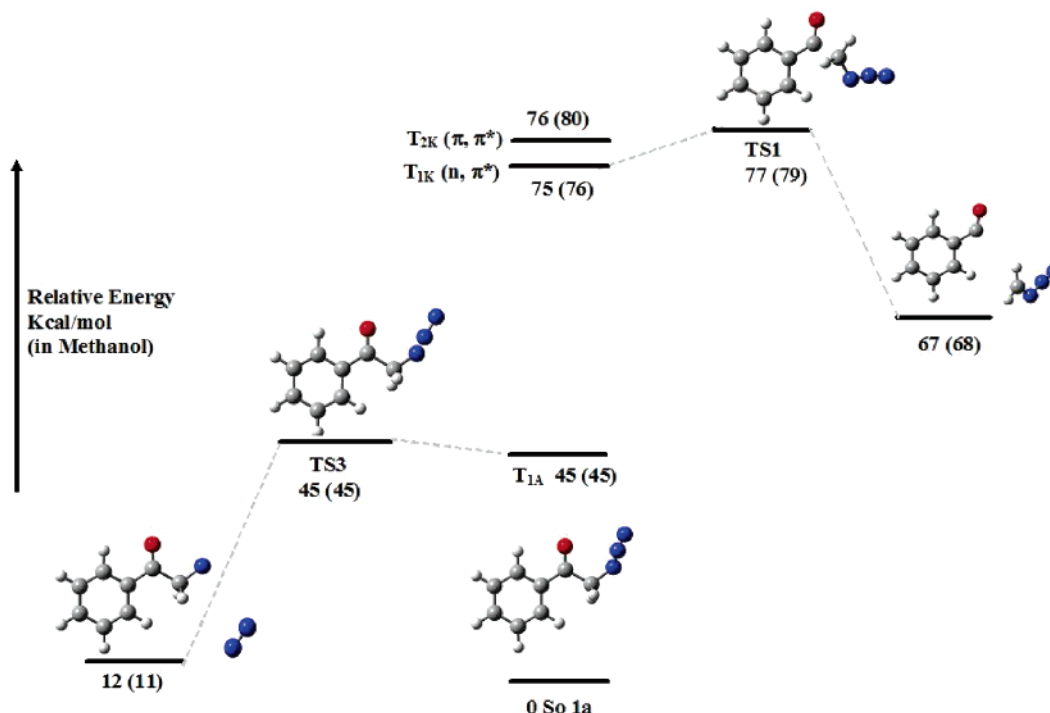


FIGURE 5. Calculated stationary points on the energy surface for α -cleavage and energy transfer in azide **1a** at the UB3LYP and TD-B3LYP (in parentheses) levels of theory.

We calculated the triplet transition states, **TS1** and **TS2**, for azides **1** to undergo α -cleavage to form benzoyl (PhC(=O)^\bullet) and azidomethyl ($\text{N}_3\text{CH}_2^\bullet$) radicals (Figures 5 and 6). Intrinsic reaction coordinate (IRC)²¹ calculations allowed us to correlate the (n,π^*) configuration of the triplet ketone to the benzoyl and azidomethyl radicals to these transition states. The transition states for α -cleavages are located only about 2 kcal/mol above the triplet ketones with (n,π^*) configuration in azides **1**. Thus, the α -cleavage is easily accessible from T_{1K} in azides **1a,b** at room temperature; however, the initial population of T_{2K} in azide **1b** does not appear feasible. The energy gap between T_{1K} and T_{2K} in azide **1b** is too large for them to be in equilibrium or to be strongly mixed with each other. Furthermore, intersystem crossing from the first excited singlet state in azide **1b** can populate either T_{1K} or T_{2K} , but internal conversion to T_{1K} is expected to depopulate T_{2K} efficiently.

We also calculated the triplet transition states, **TS3** and **TS4**, for formation of triplet nitrenes **2** from the azides **1a,b** (Figures

5 and 6). IRC calculations correlated the triplet azides and triplet nitrenes with these transition states. The transition state for the triplet azides falling apart to yield triplet nitrene intermediates is less than 1 kcal/mol above the transition state, indicating that the triplet azides must be short-lived intermediates. The energy transfer to the azido moiety must come from the (π,π^*) triplet ketones in azides **1a,b**. Thus, we expect both azides **1a** and **1b** to undergo energy transfer since T_{1K} in azide **1b** has a (π,π^*) configuration and because T_{2K} (π,π^*) in azide **1a** is close in energy to T_{1K} (n,π^*) and could be in equilibrium with each other.

Finally, we calculated the transition states, **TS5** and **TS6**, for α -cleavage of nitrenes **2** to form the corresponding benzoyl radical **3** and methylene iminyl radical. These transition states were also connected to the respective reactant and products by IRC calculation. Stationary points on the triplet energy surface for the α -cleavage of nitrenes **2** are shown in Figures 7 and 8. The transition states are located about 18 kcal/mol above the ground state of nitrenes **2**. Thus, at ambient temperature we expect nitrenes **2** to undergo α -cleavage to form benzoyl radicals **3**, since this is a rearrangement of the ground state of the triplet nitrenes. More

(20) Srinivasan, A.; Kebede, N.; Saavedra, J. E.; Nikolaitchik, A. V.; Brady, D. A.; Yourd, E.; Davies, K. M.; Keefer, L. K.; Toscano, J. P. *J. Am. Chem. Soc.* **2001**, *123*, 5465.

(21) (a) Gonzalez, C.; Schlegel, H. B. *J. Chem. Phys.* **1989**, *90*, 2154. (b) Gonzalez, C.; Schlegel, H. B. *J. Phys. Chem.* **1990**, *94*, 5523.

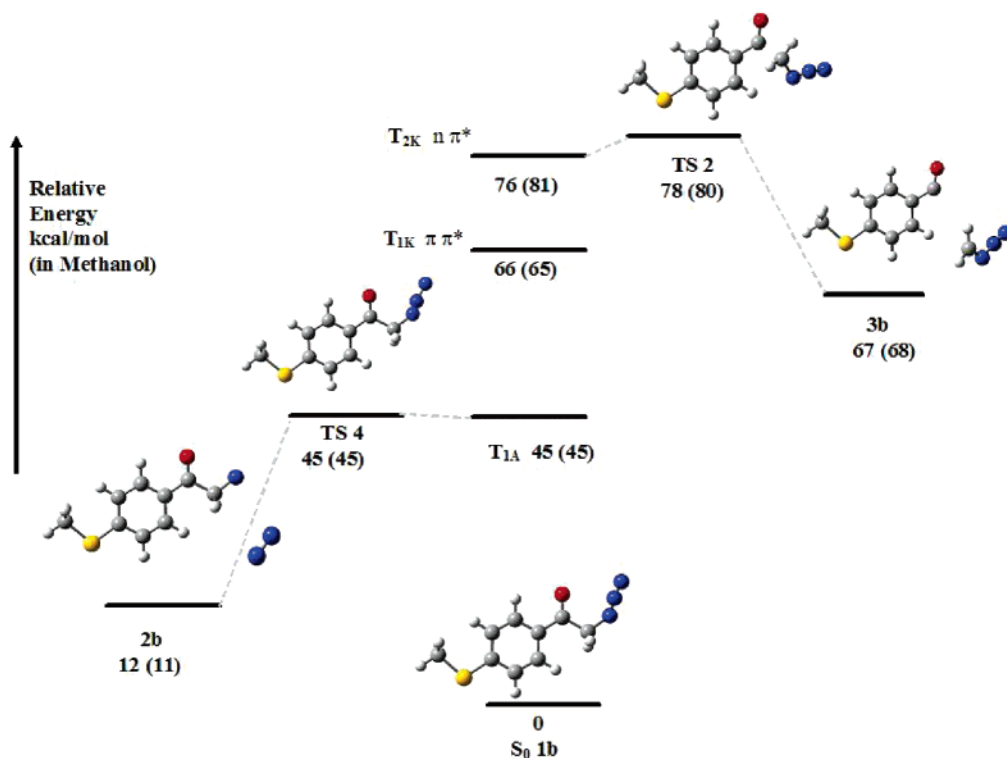


FIGURE 6. Calculated stationary points on the energy surface for α -cleavage and energy transfer for azide **1b** at the UB3LYP and TD-B3LYP (in parentheses) levels of theory.

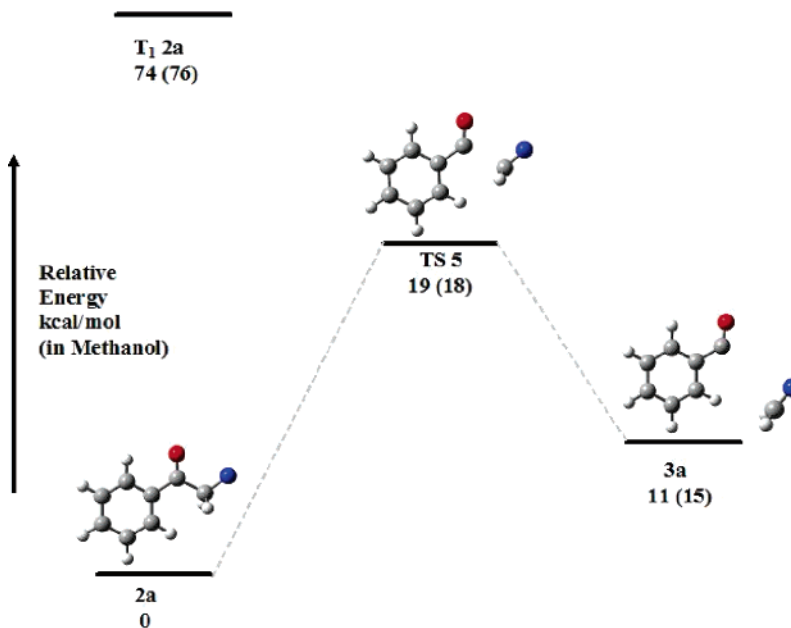


FIGURE 7. Calculated stationary points on the triplet energy surface for α -cleavage of nitrene **1a** at the UB3LYP and TD-B3LYP (in parentheses) levels of theory.

specifically, either the nitrene or the ketone chromophores in nitrenes **2** can absorb light and decay back to a vibrationally hot ground state, which can then fall apart to yield benzoyl and iminyl radicals.

D. Laser Flash Photolysis. Laser flash photolysis (excimer, $\lambda = 308$ nm, 17 ns) of azide **1b** in nitrogen-saturated methanol produces a transient absorption signal with λ_{max} at 450 nm due to absorption of its triplet ketone, which decays with a rate of

$2.1 \times 10^5 \text{ s}^{-1}$ (Figure 9). Simultaneously with this decay, a new transient with λ_{max} at 320 nm forms with the same rate constant as the triplet ketone decays, and we assign the 320 nm absorption to the triplet nitrene **2b** (Figure 11). We base this assignment on the similarity of this transient to the calculated absorption spectra of **2b**. TD-B3LYP calculations predict that nitrene **2b** has absorption bands in methanol at 450 ($f = 0.0038$), 399 ($f = 0.040$), 358 ($f = 0.035$), 322 ($f = 0.203$),

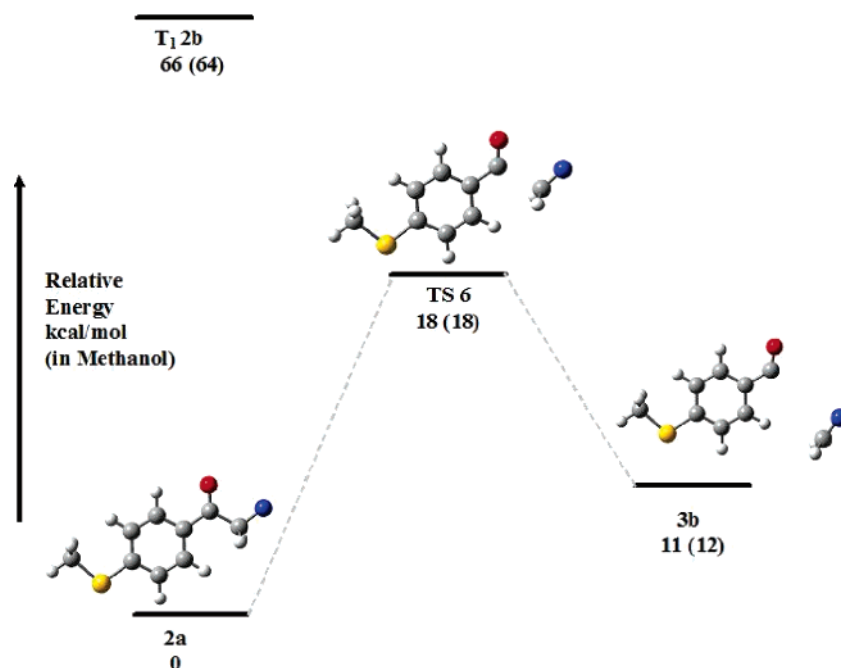


FIGURE 8. Calculated stationary points on the triplet energy surface for α -cleavage of nitrene **1b** at the UB3LYP and TD-B3LYP (in parentheses) levels of theory.

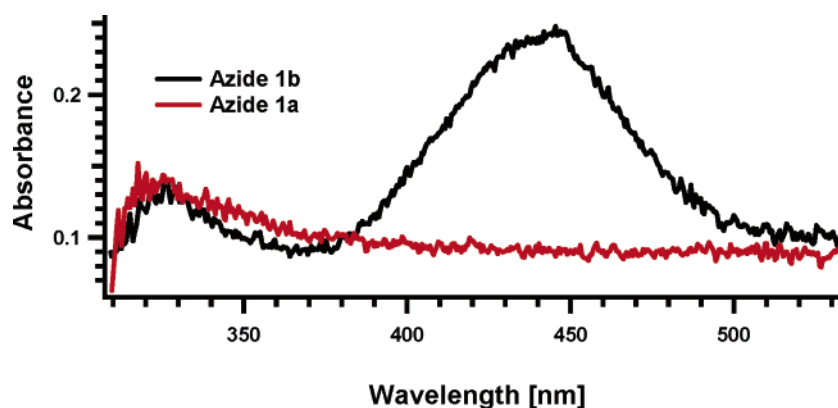


FIGURE 9. Laser flash photolysis (308 nm) of azides **1a** and **1b** in nitrogen-saturated methanol right after the laser pulse in a 300 ns window.

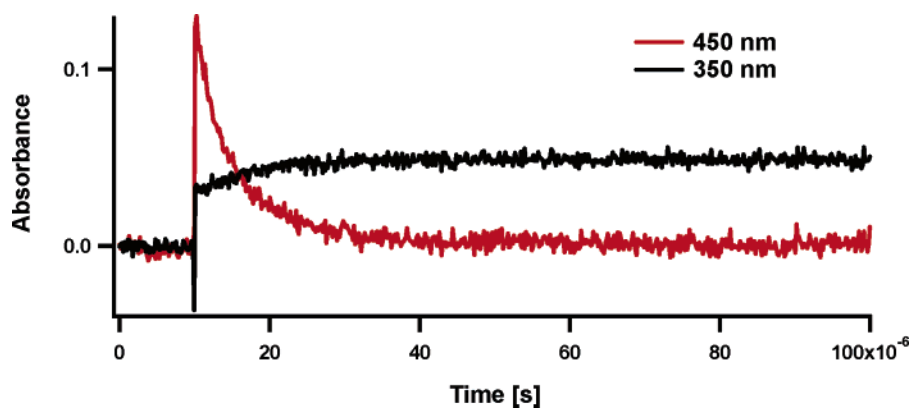


FIGURE 10. Decay of T_{1K} in **1b** at 450 nm, and formation of **2b** at 350 nm.

and 320 nm ($f = 0.241$). The band at 450 nm comes mainly from an electronic transition from the lone pair on the sulfur atom into the π^* orbital, whereas the 399 nm transition is mainly due to an electronic transition out of the π -orbitals into the half-

full orbital on the nitrogen atom. The bands around 320 nm are mixed transitions out of the lone pair on the sulfur and oxygen atoms as well as the half-full orbitals on the nitrogen atom and into the π^* orbitals. In oxygen-saturated ethanol solution, the

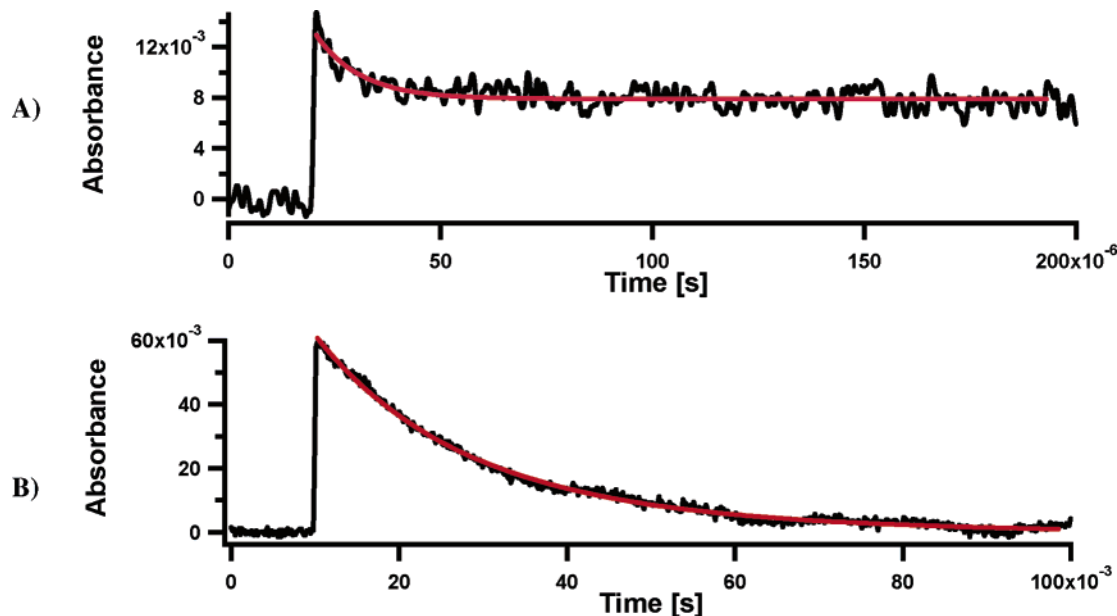


FIGURE 11. Decay at 350 nm of (a) benzoyl radical **3a** and (b) nitrene **2a** after initial laser flash photolysis of **1a** ($\lambda = 308$ nm) in nitrogen-saturated methanol.

triplet ketone absorption is quenched and the yield of the nitrene absorption is decreased, but the appearance of the spectra is not affected (see Supporting Information), which confirms that benzoyl radical **3b** is not formed upon direct photolysis of **1b**. Benzoyl radical **3b** is expected to be quenched efficiently with molecular oxygen as **3a**.^{4a} Benzoyl radical **3b** and nitrene **2b** are expected to have different absorption spectra (see Table 1); thus, if **3b** is formed from **1b**, laser flash photolysis of **1b** oxygen-saturated ethanol should yield a different transient spectrum than in argon-saturated ethanol. Thus, the laser flash photolysis data show that benzoyl radicals **2b** are not formed from photolysis of azide **1b**. Furthermore, in air-saturated methanol solutions, the rate of decay for the triplet ketone is $1.5 \times 10^7 \text{ s}^{-1}$ (Figure 10). The decay of alkyl nitrene **2b** in nitrogen-saturated methanol can be followed on the millisecond time scale and fitted with first-order decay to be 64 s^{-1} . In air- and oxygen-saturated methanol solution, the decay rates for **2b** are 150 and 250 s^{-1} , respectively. By assuming that the oxygen concentration at saturation is 0.01 M in methanol,¹⁰ we can estimate that nitrene **2b** reacts with oxygen with a rate constant of $3 \times 10^4 \text{ M}^{-1} \text{ s}^{-1}$. In comparison, Liang and Schuster reported that triplet *p*-nitrophenyl nitrene reacts with oxygen with a rate of less than $2 \times 10^5 \text{ M}^{-1} \text{ s}^{-1}$ whereas Gritsan and Pritchina estimate this same rate constant to be somewhat larger.^{23,24} This rate is, however, in agreement with computational work by Liu et al., who reported that triplet alkyl nitrenes can be expected to react similarly with oxygen as do triplet phenyl nitrenes.²⁵ This is in contrast to Toscano and co-workers, who reported much faster bimolecular reactions ($\sim 10^9$) for molecular oxygen reacting with triplet benzyloxynitrene ($^3\text{PhCH}_2\text{ON}$),²⁰ but Liu

et al. ascribed this unusual reactivity to an electron-transfer component in this nitrene class.²⁵

We previously reported that the laser flash photolysis of azide **1a** results in a broad absorption band that has a maximum around 320 nm.^{4a} The calculated spectrum of nitrene **2a** in methanol has predicted peaks at 355 ($f = 0.014$) and 308 nm ($f = 0.024$), and these features agree well with the observed transient absorption. Additionally, laser flash photolysis ($\lambda = 308$ nm) of azide **1a** also shows formation of benzoyl radical **3a** concurrently with that of nitrene **2a**. Benzoyl radical **3a** has been reported to have a weak absorption at ~ 370 nm.²⁶ The calculated absorption spectrum of benzoyl radical supports this (see Table 2). We do not observe the triplet ketone in azide **1a** because the energy of the triplet ketone is higher than in **1b**; thus, it is more efficiently quenched by energy transfer and α -cleavage. We previously estimated the lifetime of triplet ketone in azide **1a** to be between 0.9 and 0.09 ns.^{4a} The rate for the decay of the benzoyl radical **3a** can be measured at 350 nm to be around $2 \times 10^5 \text{ s}^{-1}$, whereas the nitrene **2a** decays with a unimolecular rate constant of 91 s^{-1} (Figure 11).

The laser flash photolysis of azides **1** demonstrates that azide **1a** forms both benzoyl radical **3a** and nitrene **2a** whereas **1b** only forms nitrene **2b** since we did not observe any decay that can be attributed to benzoyl radical **3b**.

E. Effect of Concentration on the Product Ratio. We irradiated five different concentrations of azides **1** in toluene with a continuous-wave, argon-ion laser¹¹ ($\lambda = 351$ nm) and analyzed the product ratios using HPLC chromatography. In Figure 11, the ratio of $([\mathbf{4}] + [\mathbf{5}] + 2[\mathbf{6}])/([\mathbf{4}] + [\mathbf{7}])$ was plotted versus the concentration of azides **1**. Products **4**, **5**, and **6** are attributed to formation of benzoyl radical **3**, whereas products **4** and **7** are due to formation of triplet alkyl nitrene **2**. We count product **6** twice because it is due to dimerization of two benzoyl radicals. Since product **4** results from both benzoyl radical **3** and nitrene **2**, we count it as both the benzoyl radical and

(22) (a) Singh, P. N. D.; Mandel, S. M.; Sankaranarayanan, J.; Muthukrishnan, S.; Chang, M.; Robinson, R. M.; Ault, B. S.; Gudmundsdottir, A. D. Unpublished work. (b) Sankaranarayanan, J.; Mandel, S. M.; Krause, J. A.; Gudmundsdottir, A. D. *Acta. Crystallogr., Sect. E* **2007**, E63, o721.

(23) Liang, T.-Y.; Schuster, G. B. *J. Am. Chem. Soc.* **1987**, 109, 7803.

(24) (a) Gritsan, N. P.; Pritchina, E. S. *J. Inf. Rec. Mater.* **1989**, 17, 391.

(b) Pritchina, E. A.; Gritsan, N. P. *J. Photochem. Photobiol. A* **1988**, 43, 165.

(25) Liu, J.; Hadad, C. M.; Platz, M. S. *Org. Lett.* **2005**, 7, 549.

(26) Huggenberger, C.; Lipscher, J.; Fischer, H. *J. Phys. Chem.* **1980**, 84, 3467.

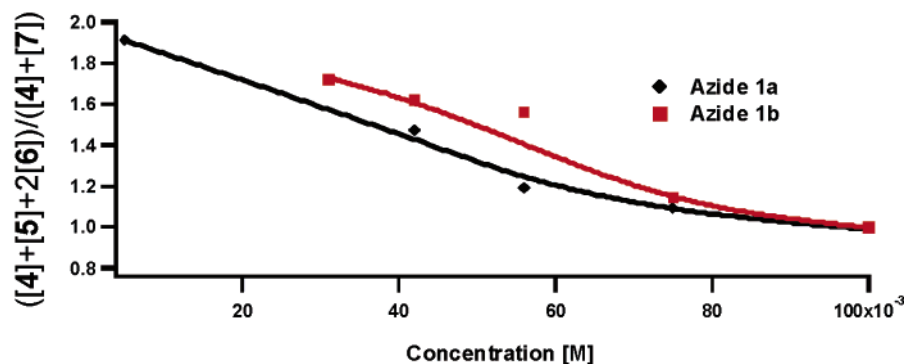


FIGURE 12. Effect of concentration on product ratio for azides 1.

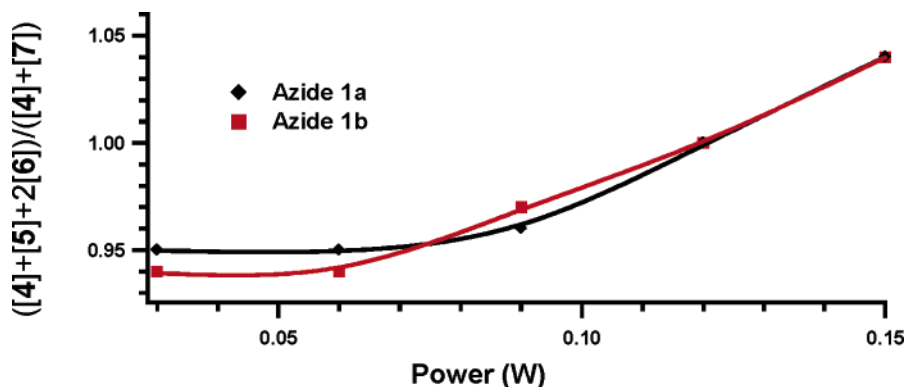
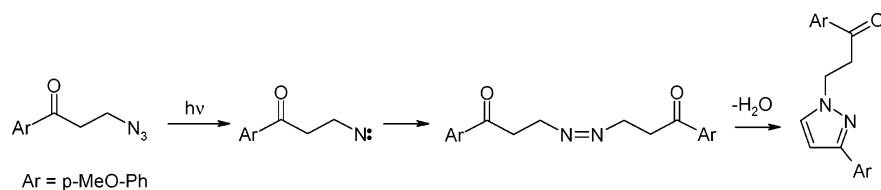


FIGURE 13. Effect of light intensity on product ratio from azides 1.

SCHEME 6



nitrene-based products. As more is formed of **3** and less of **2** from **1** the ratio of $[4] + [5] + 2[6]$ versus $[4] + [7]$ will increase. This ratio also increases when more of **2** cleaves to form **3**. Both azides **1a** and **1b** yield more products attributed to benzoyl radical formation at lower concentration, which supports the notion that nitrenes **2a,b** both cleave to form benzoyl radicals **3a,b**. Formation of nitrenes **2** in less concentrated solution makes it more likely that they can fall apart photochemically to form **3** before the nitrenes scavenge other radicals. Since the product ratios are similar for both azides **1a** and **1b**, it is likely that benzoyl radicals **3** are mainly formed from cleavage of nitrenes **2**.

F. Product Ratios as a Function of Light Power. We irradiated toluene solutions of azides **1a,b** with a high-intensity, continuous-wave, argon-ion laser at five different laser powers and analyzed the product ratios. In Figure 12 we plot the product ratio $([4] + [5] + 2[6]) / ([4] + [7])$ as a function of the laser power. As the power of the light source was increased, this ratio increased slightly for both azides **1a** and **1b**, which indicates that more of benzoyl radical-based products are formed. These findings also support the idea that nitrenes **2** can form benzoyl radical **3** photochemically.

III. Discussion

TD-B3LYP calculations confirm that $T_{1K} (n, \pi^*)$ and $T_{2K} (\pi, \pi^*)$ are almost degenerate in azide **1a**. Laser flash photolysis of azide **1a** shows that benzoyl radical **3a** and nitrene **2a** are formed, presumably from T_{1K} and T_{2K} , respectively. Although UB3LYP optimizations with the 6-31+G(d) basis set underestimates the energy of T_{1K} in azide **1a** by ~ 9 kcal/mol, this theoretical method does demonstrate that the transition state for the α -cleavage is only a few kcal/mol above T_{1K} . The α -cleavage in azide **1a** is facilitated by the radical stabilization energy of the azido group. We have shown that azido substituents have a radical stabilization energy of 15 kcal/mol, which is similar to that observed for phenyl and alkenyl substituents.²⁷ In comparison, laser flash photolysis of azide **1b** shows only formation of nitrene **2b**, which comes from energy transfer from T_{1K} to the azido group. As $T_{2K} (n, \pi^*)$ is 10 kcal/mol higher in energy than $T_{1K} (\pi, \pi^*)$ in azide **1b**, the (n, π^*) state is not effectively populated at ambient temperature, and therefore, we do not observe any benzoyl radical formation upon laser flash photolysis of azide **1b**.

(27) Mandel, S. M.; Singh, P. N. D.; Muthukrishnan, S.; Chang, M.; Krause, J. A.; Gudmundsdottir, A. D. *Org. Lett.* **2006**, 8, 4207.

Laser flash photolysis demonstrates that triplet alkylnitrenes **2** are long-lived intermediates. Furthermore, we have previously shown that triplet alkylnitrenes are highly unreactive and prefer to dimerize with another nitrene molecule rather than react with an azide precursor (Scheme 6),²² and Schuster et al. reported similar findings for phenylnitrene intermediates.²³ Alkylnitrenes owe their stability to the fact that they are unreactive to H-atom abstraction from the solvent and react very slowly with O₂.²² Thus, alkylnitrenes decay mainly by dimerization unless they are formed in the presence of radicals with which they can react. Since photolysis of azide **1a** forms triplet nitrene **2a** and benzoyl radical **3a** simultaneously, it is reasonable to assume that the triplet alkylnitrene **2a** intercepts benzoyl radical **3a** to form the major product **4**. Since product studies for azides **1b** also yield **4** as the major product, even though laser flash photolysis does not indicate formation of benzoyl radical **3b**, we theorized whether nitrenes **2** could undergo α -cleavage to form benzoyl and iminyl radicals. Since, nitrenes **2** are long-lived and absorb light above 300 nm, it is reasonable that they could absorb a photon and undergo secondary photolysis to form benzoyl and iminyl radicals. Molecular modeling shows that the transition state for this cleavage is located 18 kcal/mol above the ground state of nitrene **2a**, and therefore at ambient temperature, it most likely takes place photochemically rather than thermally. In comparison to azides **1a,b** where only azide **1a** can undergo α -cleavage, both nitrenes **2a** and **2b** are expected to undergo α -cleavage because it is a ground-state reactivity for the alkylnitrenes. Thus, one hypothesis is that the ketone or the nitrene chromophores in nitrenes **2** can absorb light and then decay to a vibrationally hot ground state of nitrenes **2**, which falls apart to give benzoyl and iminyl radicals. Similarly, Platz et al. have shown that phenylnitrenes are also photolabile.^{2,28}

Additionally, the hypothesis that nitrenes **2** are photoreactive themselves is further supported by the fact that increases in the laser power can produce slightly more of the products derived from benzoyl radical formation. Moreover, as the concentration of the azide precursor decreases, more benzoyl radical products are observed, presumably because at lower concentration nitrenes **2** are not intercepted as efficiently in a bimolecular reaction with other radicals and can therefore efficiently absorb light to subsequently fall apart.

IV. Conclusions

Laser flash photolysis of azide **1a** produces nitrene **2a** and benzoyl radical **3a**, whereas azide **1b** yields only nitrene **2b**. Molecular modeling demonstrates that T_{1K} (n,π^*) and T_{2K} (π,π^*) are almost degenerate in azide **1a** and that T_{1K} undergoes α -cleavage to form benzoyl radical **3a**, whereas energy transfer from T_{2K} to the azido moiety forms nitrene **2a**. In comparison, T_{1K} (π,π^*) in azide **1b** is estimated to be 10 kcal/mol lower in energy than T_{2K} (n,π^*), and thus, we do not observe any α -cleavage from azide **1b**. However, we suggest that both nitrenes **2a** and **2b** undergo photochemical α -cleavage to form benzoyl radicals **2**. This notion was further supported by molecular modeling and product studies.

V. Experimental and Computational Methods

Calculations. All geometries were optimized as implemented in the Gaussian03 programs at the B3LYP level of theory and with the 6-31+G(d) basis set.^{12,13} All transition states were located at

the UB3LYP level of theory, and each transition state was confirmed to have one imaginary vibrational frequency by analytical determination of the second derivatives of the energy with respect to internal coordinates. IRC calculations were used to verify that the located transition states corresponded to the attributed reactant and product. Vertical UV absorption spectra were calculated at the TD-B3LYP level with the 6-31+G(d) basis set using the optimized B3LYP/6-31+G(d) geometry for the S₀ state. The T_{1K} of azide **1a** was optimized using UB3LYP and TD-B3LYP with the 6-31+G(d) basis set as implemented in the TURBOMOLE package. Appropriate zero-point energy (ZPE) corrections were made, and wherever it was not possible to obtain the ZPE, the uncorrected energies were compared. The effect of solvation was calculated using the self-consistent reaction field (SCRF) method with the integral equation formalism polarization continuum model (IEF-PCM)¹⁵ with methanol as the solvent.

Phosphorescence. The phosphorescence spectra were obtained on a standard phosphorimeter.

Laser Flash Photolysis. Laser flash photolysis was done with an excimer laser (308 nm, 17 ns). These systems have been described elsewhere.^{29,30} A stock solution of azides **1a** and **1b** in methanol was prepared with spectroscopic-grade methanol such that the solutions had an absorption between 0.6 and 0.8 at 308 nm. Typically, ~1 mL of the stock solution was placed in a 10 × 10 mm wide, 48 mm long quartz cuvette and purged with nitrogen for 5 min. The rates were obtained by fitting an average of 3–8 kinetic traces. The absorption spectra were measured using an excimer laser in conjunction with an optical multichannel analyzer.

Synthesis of Azide **1 and Its Photoproducts.** We previously reported the preparation of azide **1a** and its photoproducts.⁴

2-Bromo-1-(4-methylsulfanyl-phenyl) Ethanone. 2-Bromo-1-(4-methylsulfanyl-phenyl) ethanone was prepared according to the literature, and its IR and ¹H NMR are identical to those previously reported.³¹ IR (CHCl₃): 1694, 1590, 1477, 1428 cm⁻¹. ¹H NMR (250 MHz, CDCl₃): δ 2.53 (s, 3H), 4.40 (s, 2H), 7.28 (d, 8.4 Hz, 2H), 7.89 (d, 8.4 Hz, 2H) ppm.

Synthesis of 2-Azido-1-(4-methylsulfanyl-phenyl) Ethanone (1b**).** Azide **1b** was synthesized following a procedure similar to a method described by Boyer et al.³² 2-Bromo-1-(4-methylsulfanyl-phenyl) ethanone (1.3 g, 5 mmol) was dissolved in ethanol (20 mL), and glacial acetic acid (1 mL) was added while the solution was kept between 0 and 5 °C. Sodium azide (690 mg, 10 mmol) dissolved in minimum water was added, and the reaction mixture was shaken vigorously and kept at 4 °C for 12 h. The reaction mixture was extracted with diethyl ether (3 × 50 mL); the organic layer was dried over anhydrous magnesium sulfate and evaporated under vacuum. The residue was purified on a silica gel column eluted with 10% ethyl acetate in hexane to yield **1b** as pale yellow solid (786 mg, 3.8 mmol, 80% yield). This solid was recrystallized from ethanol to give crystals of **1b**. The X-ray structure analysis of **1b** revealed that its crystals were orthorhombic with a P2₁2₁2₁ space group (See Supporting Information).

Mp: 76–77 °C. IR (neat): 2106, 1690, 1590 cm⁻¹. ¹H NMR (250 MHz, CDCl₃): δ 2.53 (s, 3H), 4.52 (s, 2H), 7.28 (d, 8 Hz, 2H), 7.80 (d, 8 Hz, 2H) ppm. ¹³C NMR (400 MHz, CDCl₃): δ 192.6, 148.1, 128.9, 126.1, 125.9, 55.3, 15.3 ppm. MS (EI): *m/z* (relative intensity) 207 (M⁺, 15), 179 (21), 152 (60), 151 (100), 135 (13), 123 (77), 122 (11), 121 (14), 108 (68), 79 (52), 77 (31). HRMS: *m/z* calcd for C₉H₉OSN₃ [M + H]⁺, 207.0466; found, 207.0475. UV–vis (methanol): λ_{max} 203, 236, 309 (ϵ = 8100) nm.

Synthesis of Benzil **6b.** 1,2-Bis-(4-methylsulfanyl-phenyl)-ethane-1,2-dione was synthesized via a standard benzoin condensa-

(29) Gritsan, N. P.; Zhai, H. B.; Yuzawa, T.; Karweik, D.; Brooke, J.; Platz, M. S. *J. Phys. Chem. A* **1997**, *101*, 2833.

(30) Cosa, G.; Scaiano, J. C. *J. Photochem. Photobiol.* **2004**, *80*, 159.

(31) Rahim, A. M.; Rao, P. N. P.; Knaus, E. E. *Bioorg. Med. Chem. Lett.* **2002**, *12*, 2753.

(32) Boyer, J. H.; Straw, D. *J. Am. Chem. Soc.* **1952**, *74*, 4506. (b) Boyer, J. H.; Straw, D. *J. Am. Chem. Soc.* **1953**, *75*, 1642.

(28) Levya, E.; Platz, M. S.; Persy, G.; Wirz, J. *J. Am. Chem. Soc.* **1986**, *108*, 3783.

tion.³³ 4-Methylsulfanyl-benzaldehyde (1.54 g, 10 mmol) was dissolved in ethanol (8 mL), KCN (0.28 g, 4.3 mmol) was added, and the mixture was refluxed on a sand bath at 95 °C for 35 min. The mixture was cooled in an ice bath, and the crystals that formed were filtered, washed with water, air dried, and characterized as 2-hydroxy-1,2-bis-(4-methylsulfanyl-phenyl) ethanone.

Mp: 102–103 °C (Lit.³⁴ 102–103 °C). IR (neat): 1730 cm⁻¹.

Cu(OAc)₂ (0.1 g, 0.5 mmol) and NH₄NO₃ (5 g, 62 mmol) were dissolved in water (7 mL), and glacial acetic acid (28 mL) was added. This mixture (7 mL) was added to 2-hydroxy-1,2-bis-(4-methylsulfanyl-phenyl) ethanone, and the resulting solution was refluxed at 140 °C for 1 h. The mixture was cooled in an ice bath, and the solid that formed was filtered and purified on a short silica column eluted with dichloromethane. The solid was recrystallized from ethanol to yield (930 mg, 3.07 mmol, 62% yield) shiny yellow crystals of 1,2-bis-(4-methylsulfanyl-phenyl)-ethane-1,2-dione **6b**.

Mp: 161–163 °C (Lit.³⁴ 161–164 °C). IR (neat): 2970, 1654, 1537 cm⁻¹. ¹H NMR (400 MHz, CDCl₃): δ 2.52 (s, 6H), 7.27 (d, 8 Hz, 4H), 7.84 (d, 8 Hz, 4H) ppm. ¹³C NMR (100 MHz, CDCl₃): δ 193.5, 148.8, 130.1, 129.2, 125.2, 14.6 ppm. HRMS: *m/z* calcd for C₁₆H₁₄O₂S₂ [M + Na]⁺, 325.0333; found, 325.0331.

Preparative Photolysis of Azide 1b. An argon-purged solution of **1b** (300 mg, 1.4 mmol) in toluene (60 mL) was irradiated with a medium-pressure Hg arc lamp through a Pyrex filter for 14 h. HPLC analysis of the reaction mixture showed complete decomposition of **1b** and formation of a single major product **4b** and minor amounts **5b** and **7b**. The solvent was removed under vacuum, and the resulting oil was purified on a silica column eluted with 20% ethyl acetate in hexane to obtain 4-methylsulfanyl-*N*-[2-(4-methylsulfanyl-phenyl)-2-oxo-ethyl]-benzamide (**4b**) as a viscous liquid (145 mg, 0.44 mmol, 63% yield).

IR (CHCl₃): 3364, 2834, 1633, 1591 cm⁻¹. ¹H NMR (250 MHz, CDCl₃): δ 2.53 (s, 3H), 2.54 (s, 3H), 4.90 (d, 4 Hz, 2H), 7.30 (m, 4H), 7.80 (d, 8 Hz, 2H), 7.93 (d, 8 Hz, 2H) ppm. ¹³C NMR (250 MHz, CDCl₃): δ 193.8, 188.8, 167.4, 131.2, 130.6, 129.0, 128.7, 128.2, 126.1, 125.8, 47.3, 15.7, 15.3 ppm. MS (EI): *m/z* (relative intensity) 331 (M⁺, 17), 313 (100), 299 (5), 298 (25), 243 (6), 211 (5). HRMS: *m/z* calcd for C₁₇H₁₇O₂S₂N [M + H]⁺, 331.0701; found, 331.0699.

Concentration Affect on the Product Ratio from Photolysis of Azide 1a. Five different concentrations of azide **1a** (0.100, 0.07, 0.05, 0.04, 0.03 M) in freshly distilled toluene were sealed in Pyrex tubes after purging the solution with argon for 15 min. These

samples were photolyzed with a 450 W mercury arc lamp for 2 h and analyzed by HPLC. A similar set of samples was also irradiated with an argon-ion laser source for 30 min. The conversion was kept below 20%. The HPLC traces showed formation of photoproducts **4a**, **5a**, **6a**, and **7a** as well as remaining starting material. Standards for all compounds were available either commercially or from previous experiments.⁴ Similar product ratios were observed when azide **1** was photolyzed with a 450 W mercury arc lamp and a continuous wave argon-ion laser.

Concentration Affect on the Product Ratio from Photolysis of Azide 1b. Five different concentrations of azide **1b** (0.100, 0.07, 0.05, 0.04, 0.03 M) in freshly distilled toluene were sealed in Pyrex tubes after purging the solution with argon for 15 min. The samples were then photolyzed with argon-ion laser⁷ source for 30 min and analyzed by HPLC. The conversion was kept below 20%. The HPLC traces showed formation of photoproducts **4b**, **5b**, **6b**, and **7b** as well as remaining starting material. The photoproducts were characterized by injections of authentic samples. Compounds **5b** and **7b** are commercially available, whereas **6b** was synthesized as described above. Photoproduct **4b** was isolated from preparative photolysis of azide **1b**.

Effect of Light Intensity on Product Ratios Upon Irradiation of Azides 1. Five samples of 0.1 M solutions of each of azides **1** in freshly distilled toluene were sealed in Pyrex tubes after being flushed with argon for 15 min and irradiated with an argon laser light source of five different light intensities (0.03, 0.06, 0.09, 0.12, 0.15 W) for 30 min. The conversion was maintained below 20% in all instances. The product ratios (4, 5, 6, and 7) were analyzed by comparing with the standards available by normal-phase HPLC with ethyl acetate:hexane (from 0% ethyl acetate to 40%) as eluant and UV detection.

Acknowledgment. We thank the National Science Foundation, Petroleum Research Foundation, and the Ohio Supercomputer Center for supporting this work. We also thank Professor M. S. Platz at The Ohio State University and Professor J. C. Scaiano at the University of Ottawa for use of their laser flash photolysis instruments. We are grateful to Professor R. M. Wilson at the University of Cincinnati for allowing us to use his argon-ion laser.

Supporting Information Available: Cartesian coordinates, energies, vibrational frequencies, spectra of photoproducts, and CIF files for X-ray. This material is available free of charge via the Internet at <http://pubs.acs.org>.

JO062160K

(33) Mayo, D. W.; Pike, R. M.; Trumper, P. K. *Microscale Organic Laboratory*, 4th. Ed.; John Wiley & Sons: New York, 2000.

(34) Lombardino, J. G.; Wiseman, E. H. *J. Med. Chem.* **1974**, *17*, 1182.